Zhang, Y., Sachs, T., Changsheng, L., Boike, J. (2012): Upscaling methane fluxes from closed chambers to eddy covariance based on a permafrost biogeochemistry integrated model. - Global Biochemical Cycles, 18, 4, 1428-1440

DOI: 10.1111/j.1365-2486.2011.02587.x

Received Date : 17-Oct-2011
Revised Date : 17-Oct-2011
Accepted Date : 18-Oct-2011
Article type : Primary Research Articles

Running Title: Model Upscaling CH_4 Fluxes

Upscaling methane fluxes from closed chambers to eddy covariance based on a permafrost biogeochemistry integrated model

Yu Zhang [1], Torsten Sachs [2], Changsheng Li [3], Julia Boike [4]

[1] Canada Centre for Remote Sensing, Natural Resources Canada, 588 Booth Street, Ottawa, ON, K1A 0Y7, Canada
[2] GFZ German Research Centre for Geosciences, Telegrafenberg, 14473 Potsdam, Germany
[3] Complex Systems Research Center, Institute for the Study of Earth, Oceans, and Space, University of New Hampshire, 39 College Road, Durham, NH 03824-3525, USA
[4] Research Unit Potsdam, Alfred Wegener Institute for Polar and Marine Research, Telegrafenberg A43, D-14473, Potsdam, Germany

Submitted to: *Global Change Biology*

Contact for readers after published

Changsheng Li, Ph.D.
Research Professor
Complex Systems Research Center
Institute for the Study of Earth, Oceans, and Space
University of New Hampshire
39 College Road
Durham, NH 03824-3525
USA
Tel: (603) 862-1771
Fax: (603) 862-0188
Email: changsheng.li@unh.edu

This is an Accepted Article that has been peer-reviewed and approved for publication in the *Global Change Biology*, but has yet to undergo copy-editing and proof correction. Please cite this article as an "Accepted Article"; doi: 10.1111/j.1365-2486.2011.02587.x

Contact for the editor during publishing process

Yu Zhang, Ph.D.
Research Scientist
Canada Centre for Remote Sensing
Natural Resources Canada
588 Booth Street
Ottawa, ON K1A 0Y7
Canada
Tel: (613) 947-1367
Fax: (613) 947-1385
Email: yu.zhang@ccrs.nrcan.gc.ca

Abstract

Northern peatlands are a major natural source of methane (CH_4) to the atmosphere. Permafrost conditions and spatial heterogeneity are two of the major challenges for estimating CH_4 fluxes from the northern high latitudes. This study reports the development of a new model to upscale CH_4 fluxes from plant communities to ecosystem scale in permafrost peatlands by integrating an existing biogeochemical model (DNDC) with a permafrost model (NEST). A new ebullition module was developed to track the changes of bubble volumes in the soil profile based on the ideal gas law and Henry's law. The integrated model was tested against observations of CH_4 fluxes measured by closed chambers and eddy covariance method in a polygonal permafrost area in the Lena River Delta, Russia. Results from the tests showed that the simulated soil temperature, summer thaw depths and CH_4 fluxes were in agreement with the measurements at the five chamber observation sites; and the modeled area-weighted average CH_4 fluxes were similar to the eddy covariance observations in seasonal patterns and annual totals though discrepancy existed in shorter time-scales. This study indicates that the integrated model, NEST-DNDC, is capable of upscaling CH_4 fluxes from plant communities to larger spatial scales.

Key words: methane flux, model, permafrost, upscale, peatland, DNDC, NEST.

1. Introduction

Methane (CH_4) is an important greenhouse gas in the atmosphere responsible for about 22% of the presently enhanced greenhouse effect (Lelieveld *et al.* 1998). Wetlands are the largest natural source of atmospheric CH_4, contributing 110 - 260 Tg of CH_4 per year to the global CH_4 budget (Prather *et al.* 2001), a quarter to a third of which is emitted from the wet soils of high latitudes (Walter *et al.* 2001). Northern peatlands have accumulated 547 Gt of carbon since the Last Glacial Maximum (Yu *et al.* 2010) and most northern peatlands are associated with permafrost (Tarnocai *et al.* 2009). Climate warming at high latitudes was about twice the global average during the 20th century, and climate models projected that this pattern will continue during the 21st century. Climate warming directly affects active-layer thickness and permafrost distribution, which could alter hydrological conditions as well. These changes in soil thermal and hydrological conditions may cause the release of the soil carbon stock as greenhouse gases, especially as CH_4, further enhancing climate warming (Frolking *et al.* 2010).

Northern peatlands are strongly heterogeneous, with hollows, hummocks, lawns, and pools, associated with tussocks, polygons, and local collapse of permafrost. CH_4 fluxes could differ by one to two orders of magnitude in a distance of meters (Whalen *et al.*

1991; Morrissey & Livingston 1992; Bubier *et al.* 1993; Sachs *et al.* 2010). Therefore it is important to consider the effects of the spatial heterogeneity in estimating regional CH_4 fluxes (Dinsmore *et al.* 2009). Upscaling from local scale to regional or global scales is one of the major challenges in quantifying the impacts of northern peatlands on the climate system (Frolking *et al.* 2010). Several studies have upscaled CH_4 fluxes based on site observations of CH_4 fluxes from different land types (e.g. Matthews & Fung 1987; Whalen *et al.* 1991; Schneider *et al.* 2009). Although this approach can specify the spatial differences, field observations are costly and can only cover very limited sites and time periods. Process-based models can integrate biophysical and biogeochemical processes to understand and estimate CH_4 fluxes in different conditions. Most model estimations of CH_4 fluxes for regional and global scales used half-degree latitude/longitude or coarser spatial resolutions without considering the effects of local spatial heterogeneity (e.g., Cao & Marshall 1998; Walter *et al.* 2001; Zhuang *et al.* 2004). Therefore it is important to develop a method to understand the effects of local spatial heterogeneity in spatial modeling and regional estimation.

CH_4 fluxes have been measured using closed chambers at many locations in the last two decades (e.g., Bubier *et al.* 1993). Closed chambers can be put in different plant communities and the observations represent CH_4 fluxes at a scale of a few meters. CH_4 fluxes can also be observed using eddy covariance (EC) techniques. Depending on the heights of the towers, the EC observations represent CH_4 fluxes at a scale of several hectares to about a square kilometer. Following the terms used by Riutta *et al.* (2007), we referred to the scales represented by the chambers and EC observations as the plant community scale and the ecosystem scale, respectively. Plant communities are land units with separable and distinct plant conditions, water table behavior, regimes of net peat accumulation, and relatively uniform ecohydrological and biogeochemical processes. Therefore plant communities are the basic scale for upscaling to ecosystem or larger scales.

Since ecosystem scale CH_4 fluxes can be estimated using chamber observations at different plant communities in the ecosystem, several studies compared the upscaled CH_4 fluxes with the observations by EC techniques (Heikkinen *et al.* 2006; Riutta *et al.* 2007; Hendriks *et al.* 2010; Sachs *et al.* 2010; Schrie-Uijl *et al.* 2010). Spatial upscaling is based on the areal fractions of the plant communities within the footprint of the towers. Since chamber observations were not conducted continuously, regression equations were used to upscale temporally. Most of these studies found that the upscaled CH_4 and/or CO_2 fluxes agreed with the observations of the EC techniques in monthly or seasonal totals (Riutta *et al.* 2007; Sachs *et al.* 2010; Schrie-Uijl *et al.* 2010) although no studies explicitly compared the upscaled and EC observed CH_4 fluxes at a daily time-scale. All these studies show that spatial heterogeneity is important for upscaling CH_4 fluxes, and the regression models developed based on chamber observed CH_4 fluxes and biophysical variables were different among plant communities and study areas.

The purpose of this study is to develop a process-based model to quantify CH_4 fluxes in permafrost conditions. To explicitly consider spatial heterogeneity, we used the ecosystem scale as the spatial domain of the model. An ecosystem can be composed of a number of plant communities. The model simulates the biophysical and biogeochemical processes in each plant community and upscales to the ecosystem scale based on the areal fractions of the plant communities in the ecosystem. Thus the model may be useful to understand the processes and major controls of CH_4 fluxes at the plant community scale, and to assess the gaps and uncertainties in upscaling to the ecosystem scale. The model can also be used as a tool to estimate CH_4 fluxes at large scales considering the effects of plant communities. We developed the model by integrating an existing biogeochemical model with a permafrost model. The datasets measured by Sachs and colleagues (2008a, b, 2010) with both chamber and EC methods at an experimental site in the wet polygonal tundra in the Lena River Delta, Russia, were used to test the applicability of the new model.

2. Method and Data

2.1 Model fusion

An existing biogeochemical model, DeNitrification-DeComposition or DNDC, was integrated with a permafrost model, Northern Ecosystem Soil Temperature or NEST, to gain capacity for modeling the interactions between soil thermal-hydrological conditions and biogeochemical processes in permafrost soils. The new model, NEST-DNDC, inherited the characters of its parents on soil layer structure, one-dimension mass and energy fluxes, daily climate data for input but usually with shorter time-steps in calculation. Figure 1 shows the structure of the integrated model.

The DNDC model

The DNDC model was originally developed for estimating carbon sequestration and nitrogen trace gas emissions from agricultural ecosystems (Li *et al.* 1992). Later on Li *et al.* (2000) integrated DNDC with a forest model and a nitrification model to simulate carbon and nitrogen dynamics in forest ecosystems. A kinetic scheme “anaerobic balloon” was developed to quantify the relative aeration status in soil (Li *et al.* 2000). Zhang *et al.* (2002a) further extended the model to wetland ecosystems considering water table dynamics, CH_4 fluxes, and multiple strata of vegetation, including bryophytes. The DNDC model has been validated against a wide range of observations worldwide (e.g., Li *et al.* 2002; Zhang *et al.* 2002b; Grant *et al.* 2004; Fumoto *et al.* 2008; Giltrap *et al.* 2010).

The DNDC model consists of four major components: soil climate, plant growth, soil carbon and nitrogen dynamics. The soil climate component calculates soil temperature, soil moisture, water table, and redox potential (Eh) profiles (Most of this component will be replaced by NEST during model fusion). The vegetation component calculates photosynthesis, respiration, plant growth, nitrogen uptake, and litter production. The routines simulating growth of woody plants and litter production were adopted from a forest model, PnET, developed by Aber & Federer (1992). The growth of mosses and herbaceous plants has been added in DNDC for wetland conditions (Zhang *et al.* 2002a). The component of soil carbon dynamics calculates decomposition of soil organic matter and CH_4 fluxes. The soil organic carbon (SOC) is divided into four pools (i.e., litter, microbes, humads, and passive humus), and each pool is further divided into labile and resistant fractions. The decomposition of each SOC fraction depends on its specific decomposition rate and soil thermal and moisture conditions. Methane fluxes are calculated based on CH_4 production, consumption and transport processes. Eh, temperature and pH are the major factors affecting CH_4 production and oxidation rates. Transport of CH_4 from soil to the atmosphere included plant mediated transport, ebullition and diffusion (Zhan*g et al.* 2002a). The component of soil nitrogen dynamics simulates nitrification and denitrification. The nitrification submodel predicts conversion of ammonium to nitrate with nitric oxide (NO) and nitrous oxide (N_2O) as byproducts. The denitrification submodel calculates growth and death of denitrifiers, substrate consumption, and production of nitrogen gases (i.e., NO, N_2O and N_2). Fluxes of nitrogen gases depend on their production, consumption and diffusion in the soil profile (Li *et al.* 1992, 2000).

The NEST model

NEST is a one-dimensional model simulating ground thermal dynamics and associated thawing/freezing and permafrost conditions. It also integrates snow and soil water dynamics (Zhang *et al.* 2003). Soil temperature dynamics is simulated by solving the one-dimensional heat conduction equation. The upper boundary condition (the ground surface or snow surface if snow is present) is determined by the surface energy balance; and the lower boundary condition is defined based on the geothermal heat flux. The amount of snow on the ground (water equivalent) is determined as the cumulative difference between snowfall and snow loss from snowmelt and sublimation driven by the surface energy balance. The profile of snow density is calculated considering compaction and destructive metamorphism. Soil water dynamics include water input (rainfall and snowmelt), output (evaporation and transpiration), and distribution across the soil layers. Soil thawing and freezing and associated changes in fractions of ice and water are determined based on energy conservation. Detailed description of the model has been presented by Zhang *et al.* (2003). The model has been validated against measurements of energy fluxes, snow depth, soil temperature, thaw depth, and spatial distributions of permafrost in Canada (Zhang *et al.* 2003, 2005, 2008a, 2008b). Lateral water exchange is parameterized based on an empirical approach developed for the Wetland-DNDC model (Zhang *et al.* 2002a).

Integrating NEST with DNDC

We integrated NEST with DNDC at code level to ensure that the information exchange between the two component models were precise and efficient. The new model, NEST-DNDC, is able to simulate an ecosystem domain which contains a number of plant communities. All the plant communities in the ecosystem share common weather and geological conditions but differ in their biophysical factors such as vegetation, soil and hydrology. The ecosystem-scale fluxes can be calculated by area-weighted sum of the modeled plant community scale fluxes. Inheriting from NEST, the new model simulates a deeper ground to capture the changes in summer thaw depth as well as the long-term variations of permafrost with climate. The deep ground profile also provides a stable lower boundary condition for water table simulation. The initial soil thermal and hydrological conditions for each plant community type are determined by running the model iteratively based on the climate data of the first year until the modeled annual mean soil temperature is stable.

In NEST-DNDC, the ebullition emissions of CH_4 from wetland were improved. Ebullition is an important pathway of CH_4 transport from the wetland soil to the atmosphere. The release of CH_4 in bubbles could be associated with a number of factors such as water level, barometric pressure and temperature (Fechner-Levy & Hemond 1996; Beckmann *et al.* 2004; Strack *et al.* 2005; Tokida *et al.* 2005; Kellner *et al.* 2006). Significant CH_4 emissions, probably related to the CH_4 stored in bubble form in soils, were observed during spring thaw (Moore & Knowles 1990; Hargreave*s et al.* 2001; Tokida *et al.* 2007) and early winter freezing of the summer thawed layers in permafrost regions (Sachs *et al.* 2008a; Mastepanov *et al.* 2008). Several studies explained the impacts of various factors on ebullition based on Henry's law and the ideal gas law (Fechner-Levy & Hemond 1996; Strack *et al.* 2005; Tokida *et al.* 2005; Kellner *et al.* 2006). The Wetland-DNDC model estimated ebullition as the amount of CH_4 concentration above a threshold based on the approach of Walter & Heimann (2000). In this study, we developed a new ebullition module to track the changes of bubble volumes in the soil profile and the release of CH_4 through ebullition. The new module integrates the effects of CH_4 in soil water, soil temperature, atmospheric pressure, water table, and thawing/freezing based on the ideal gas law and Henry's law. A detailed description of the module is provided in the Appendix.

By inheriting the features existing in the original NEST or DNDC model, NEST-DNDC maintains the capacity for modeling the upland and wetland ecosystems without permafrost. For example, the soil profile can include organic soil and mineral soil layers with different texture, thickness, fractions of stone/gravels and SOC content. The modeled vegetation can include an upper story and an understory of woody plants (trees or shrubs), a layer of grasses or sedges, and a layer of mosses. Thus, the model can be used for a broad range of ecosystems from forest to tundra across permafrost and non-permafrost regions.

2.2 Field measurements

The study area

The study area is located on Samoylov Island (72°22'N, 126°30'E) in the Lena River Delta, Russia (Figure 2). The delta is composed of more than 1500 islands covering about 32000 km^2. The Samoylov Island was selected for intensive study because it is considered representative of the Late Holocene terrace, which accounts for about 65% of the delta area (Are & Reimnitz 2000; Sachs *et al.* 2008a). Samoylov Island covers an area of about 5 km^2 with two different geomorphologic units: a modern floodplain in the west (2 km^2) and wet polygonal tundra in the east (3 km^2) (Sachs *et al.* 2010). The study area is located in the center of the eastern part. This region is in the continuous permafrost zone characterized by an arctic continental climate with a mean annual air temperature of -14.7 °C and mean summer precipitation of 137 mm during 1999-2005 (Boike *et al.* 2008).

The study area has a flat macro-relief with slope gradients less than 0.2% except at shores of large lakes. However, the land surface has a micro-relief due to the development of ice wedge polygons. The depressed polygon centers can be about 0.5 m lower than the polygon rims. Degradation of the polygon rims also led to the formation of small ponds. The low-center polygons usually contain some shallow water while the rims are much drier. Vegetation and soil conditions are different between polygon centers and rims as well. More detailed information about the vegetation, soil, hydrological and climatic conditions at the study area can be found in the related publications (e.g., Kutzbach *et al.* 2004; Wagner *et al.* 2005; Boike *et al.* 2008).

Field observations

The observation sites were located in the center of the eastern part of the Samoylov Island, an area with relatively homogenous wet polygons (Figure 2). CH_4 fluxes were measured using EC techniques as well as closed chambers. Successful EC measurements were conducted for 103 days from June 9 to September 19, 2006, covering an entire growing season from the middle of snowmelt to initial freezing back. Detailed description of the EC technical setup and data analysis can be found in Sachs *et al.* (2008a, 2010). Closed chamber observations of CH_4 fluxes were conducted at five representative micro-sites within the EC fetch from July 12 to September 19, 2006. Three chamber sites were in the middle of three different low-center polygons (referred to as site 1, 3, and 4. Figure 2d), one chamber site was in the middle of a high-center polygon (site 2), and one chamber site was on the rim of a low-center polygon (site 5). Three chamber collars were installed at each chamber site for replication measurements. Detailed description of the observations can be found in Sachs *et al.* (2008b, 2010). Water table was measured at the chamber observation sites as well. Other measurements at the EC system and an automatic climate station about 700 m south of the tower included air temperature, precipitation, relative humidity, solar radiation, barometric pressure, and soil temperature at various depths.

2.3 Model setup and input data

Sachs *et al.* (2010) classified the land types (or plant community types) in the study area based on a 0.5m resolution aerial image (about 600m by 600m with the chamber and EC observation sites near the center of the image). The study area can be classified into five land types: I) open water (14%), II) overgrown water (ponds with emerging plants) (14%), III) wet low-centered polygons (10%), IV) moist high-centered polygons (35%), and V) polygon rims (27%) (Sachs *et al.* 2010). These results are similar to that of Muster *et al.* (submitted) although their classification covered a larger area in this island and used finer aerial images (Their results show that the area is composed of 15% open water, 10% overgrown water, 17% wet tundra (equivalent to land type III), and 58% dry tundra (equivalent to land type IV and V)). We ran the model for these land types except the open water since the present version of NEST-DNDC does not simulate aquatic biogeochemistry of deep water.

The vegetation and soil conditions differed between the low centers and rims. About a 10 cm organic layer was accumulated at the low centers, while there was almost no organic layer on the surface of the polygon rims. The mineral soils are sandy loam and loam at the low centers and the rims, respectively. We defined the profiles of soil texture, SOC concentration, C/N ratios according to the observations by Kutzbach *et al.* (2004) and Wagner *et al.* (2005) (Table 1). The thermal conductivity of the bedrock and the geothermal heat flux were 2.8 W m^{-1} $^{o}C^{-1}$ and 0.053 W m^{-2}, respectively, based on observations at Efaghc Tiksi (71^{o}27’N, 129^{o}0’E) (Pollack *et al.* 1991). In the study, we used a soil profile of 37.8m (50 layers) to simulate soil thermal/hydrological dynamics while biogeochemical processes were simulated only for the top 0.5m (10 layers). The vegetation in the low centers is dominated by hydrophilic sedge *Carex aquatilis* and mosses. The polygon rims are dominated by mesophytic dwarf shrub *Dryas octopetatla* and mosses, with much less *Carex aquatilis* than in the low centers. We estimated the above ground biomass of the sedges, shrubs and mosses using the equations developed by Chen *et al.* (2009) based on observations of coverage and heights of the plants (Kutzbach *et al.* 2004) (Table 2).

Daily weather data (maximum and minimum air temperature, precipitation, water vapor pressure, solar radiation, wind speed and atmospheric pressure) measured by the EC tower in 2006 were used for the simulation. To extend the data, we used the measurements from an automatic meteorological station about 700 m south of the EC tower in the Samoylov Island. Some data gaps were filled using the observations at the Stolb Island weather station (about 5 km away from the study area). Snowfall was not observed at either the Samoylov station or the Stolb Island weather station after 2004. We filled these data gaps using the precipitation data during the same season but in 2002 and 2003.

To initialize the soil climate conditions, we first ran the soil thermal and hydrological sub-models of NEST-DNDC iteratively using the first year's climate data (year 1999) until the simulated annual mean soil temperature was stable. Then we proceeded with the 1999-2006 simulations using the whole span of the model's capacity including soil climate, hydrology and biogeochemistry. The hydrological parameters for modeling lateral flows were calibrated against datasets of water table observed at each chamber site in 2006 (Table 3). Since there were no water table observations for land type II (overgrown water), we calibrated the lateral flow parameters by arbitrarily assuming that the water table at this land type was about 10 cm higher than that at the lower centers (Table 3). Under flooded conditions, CH_4 fluxes increase with increase in SOC. We calibrated SOC contents for land type II by comparing the modeled CH_4 flux with the observed CH_4 flux reported by Spott (2003). To reduce the effects of simulation error of water table on soil biogeochemical processes, we used observed water table for the simulations if it was measured on that day. The modeled CH_4 fluxes from all the land types were summed up to the ecosystem scale based on their areal fractions, and then we compared this upscaled CH_4 fluxes with the observations by EC techniques.

3. Results and Analyses

3.1 Soil temperature and active-layer thickness

Figure 3 shows comparisons between modeled and observed summer thaw depth and soil temperature at different depths for the low-center and rim sites. The modeled soil temperatures were close to that of observations. Correlation coefficients at different depths ranged from 0.83 to 0.90 for the low-center site and 0.91-0.92 for the rim site (the number of samples is 101 for the two sites and the three depths). The correlation coefficients are lower at the low-center site than at the rim site, probably because the heterogeneous effects of the water conditions, mosses and roots are stronger than at the rim site. The modeled soil temperature near the surface was lower than the measurements during Aug. 28 to Sept. 10 (Day of year (DOY) 240-253), especially at the low-center site, probably because the model did not accurately capture the snowpack dynamics as well as the effects of the above surface water during this period when air temperature briefly dropped down to below freezing point.

The modeled deepening of the thaw depth followed the observations until the late growing season, during which the modeled thaw depth stayed at the ground surface for about 10 days (Figure 3c). The model results did not show thawing from the surface during this period because the near-surface temperature was slightly below 0 ^{o}C (thaw depth was defined based on soil temperature). The modeled thaw depth quickly deepened after this cold spell because most of the water in the soil profile still remained unfrozen. Thus, the discrepancy between the modeled and observed thaw depth during this cold period is an artifact of the definition of the thaw depth in the model rather than significant changes in thawing/freezing of soil water. The thawing depth in the polygon rims was shallower than that in the wet low-center because the rims were relatively drier and better insulated.

3.2 Water table and CH_4 fluxes in different land types

Figures 4a-f show the water table dynamics. Water table was simulated if there is no observation for that day, otherwise observed water table was used for that day to determine the soil water conditions. Figures 4g-l show comparisons between modeled and measured CH_4 fluxes at the five chamber observation sites. The model captured the differences among the three land types (Types III, IV and V) and their general temporal patterns of CH_4 fluxes, including some of the pulses. The seasonal CH_4 fluxes from the wet low-centers were almost one order higher than that from the moist high-center or the polygon rim. The correlations between the modeled and chamber observed daily CH_4

fluxes were significant for the three wet low-centers (Figure 5a-c). However, the correlation coefficients were negative for the two non-inundated sites (Figure 5d, 5e).

The high CH_4 emissions (50-200 mgC m^{-2} day^{-1}) from the wet low-centers were mainly due to their inundation conditions, while the temporal patterns mainly followed the changes of soil temperature, which also associated with plant growth and soil decomposition. The modeled large pulses of CH_4 flux were usually associated with the drops of water table just below the surface. The patterns and magnitudes of CH_4 fluxes modeled for the three wet low-centers (sites 1, 3 and 4) were similar to each other since their soil and vegetation conditions were assumed to be the same and the water table dynamics were similar and were above the land surface most of the season. The CH_4 fluxes at the high-center site were slightly higher than at the rim site due to its slightly wetter conditions (Figures 4d and 4e). By calibrating SOC, the modeled CH_4 fluxes from the land type II (overgrown water) were similar to the fluxes reported by Spott (2003) (The modeled average CH_4 fluxes in July and August were 31.4 and 43.8 mgC m^{-2} day^{-1}, respectively, comparing to 30.2 and 36.1 mgC m^{-2} day^{-1} reported by Spott (2003) for these two months, respectively).

3.3 Area-weighted average CH_4 fluxes at the ecosystem scale

The ecosystem-scale CH_4 emissions were calculated based on the modeled CH_4 fluxes of all the land types and their areal fractions in the study area. To include the CH_4 fluxes from the deep open water, which NEST-DNDC does not simulate, we set the CH_4 fluxes from such water bodies as 50% of the fluxes from land type II (overgrown water) based on observations from Spott (2003), whose observations show that the CH_4 flux from open water bodies, mainly through diffusion, were generally less than 8 mgC m^{-2} day^{-1}, but ebullition could contribute to an extra of 0 to 23 mgC m^{-2} day^{-1}. Figure 6 shows a comparison of the modeled area-weighted average CH_4 fluxes with the EC observed CH_4 fluxes. The magnitude and the temporal pattern of the modeled ecosystem CH_4 fluxes were similar to that of the EC observed. The modeled ecosystem CH_4 fluxes were lower than the observations in two periods, the early growing season (DOY 160-187, or June 9 to July 6) and the cold period during Sept. 9-19 (DOY 252-262). The correlation between the modeled daily ecosystem CH_4 fluxes and EC measured daily CH_4 fluxes was low, with the correlation coefficient being 0.21 (Figure 5f) or 0.34 if excluding the extremely high CH_4 flux observed on June 27 (DOY 178). However, if we compare the 3-day running averages of the modeled ecosystem CH_4 fluxes and EC observed CH_4 fluxes, the correlation coefficient increased from 0.21 to 0.42 or from 0.34 to 0.54 if excluding the extremely high CH_4 flux observed on DOY 178. The modeled total ecosystem CH_4 flux during the EC observation period (DOY 160-262, or June 9 to Sept. 19, 2006) was 1.30 gC m^{-2}, which was 10.3% less than that of the EC observations (1.45 gC m^{-2}). If we used the areal fractions classified by Muster *et al* (submitted), the modeled total ecosystem CH_4 flux was 7.2% higher than that of the EC observations, because they classified larger wet tundra.

4. Discussions

4.1 Comparing model results with observations at the chamber sites

Our modeled soil thermal dynamics and CH_4 fluxes were comparable with the observations at the chamber sites, and water table dynamics could also be simulated by calibrating the lateral water flow parameters at such scale (Figures 4a-f). These tests indicated that the one-dimensional model is suitable to quantify the thermal, hydrological, vegetation and biogeochemical processes and their interactions at the plant community scale as energy and matter fluxes (heat, radiation, water, carbon and nitrogen) and their interactions were directly connected at this scale.

Based on our model results, the annual CH_4 fluxes in 2006 were 1.6, 3.2, 5.7, 0.4, and 0.1 gC m^{-2} $year^{-1}$ from land types I to V, respectively, comparing to 1.4 gC m^{-2} $year^{-1}$ as the area-weighted average for the ecosystem scale. Land type III accounts for only 10% of the area, but contributed 40% of the CH_4 fluxes to the ecosystem. The total wet vegetated areas (land types II and III) accounted for 24% of the area but contributed 72% of the CH_4 fluxes to the ecosystem, while the high-centered polygons and rims accounted for 62% of the area but contributed to only 13% of the CH_4 fluxes. These results again emphasize that it is important to consider spatial heterogeneity in estimating CH_4 fluxes on the ecosystem scale.

In NEST-DNDC, lateral flows can be estimated by calibrating several lateral flow parameters based on water table observations. This parameterization approach provides a simplified and efficient way to capture water dynamics at the plant community scale in wetlands without explicitly considering detailed spatial features (e.g., the sizes and elevations of the plant communities, their spatial arrangement and connections, and the associated flow patterns, etc). Figure 6 shows a comparison between the modeled and observed water tables for the wet low-centered polygons (Land type III). The lateral flow parameters were calibrated as 0 for outflows and 10% for surface inflow (Table 3) (i.e., no lateral outflows, surface inflow was 10% of the rainfall or snow melt). This is reasonable because some water in the high rim can flow into the depressed polygon center while the high rim with permafrost disconnected the low center from the surrounding troughs (Sachs *et al.* 2010). We also tested this approach at a bog in northern Minnesota, USA, and it showed that the modeled water table in 39 years was consistent with the observations (Zhang *et al.* 2002a).

4.2 Comparing upscaled CH_4 fluxes with EC observations

The seasonal pattern and the magnitudes of CH_4 flux measured by EC techniques can generally be explained by the contributions of CH_4 fluxes from the different land types within the fetch of the EC tower. This conclusion is in agreement with the results of several other studies (Riutta *et al.* 2007; Sachs *et al.* 2010; Schrie-Uijl *et al.* 2010). Although we reasonably modeled CH_4 fluxes at the chamber sites, the modeled area-weighted average CH_4 fluxes did not totally match the EC observations, especially on short-time scales. Several reasons may contribute to this discrepancy.

Firstly, the chamber observation sites might not be representative enough for the different land types in the study area. Although the average and general seasonal patterns observed at the wet low-centered polygons (Site 1, 3, and 4) were similar (the average seasonal CH_4 fluxes were 58.4, 75.0 and 60.6 mgC m^{-2} day^{-1} for these three sites respectively), but the standard variations of the measurements in a day or the short-time variations were large (Sachs *et al.* 2010). There was only one observation site for land type IV and V each, and no observations for the land type I and II. Therefore the modeled or estimated CH_4 fluxes from these land types may be inaccurate, especially for land types I and II.

The CH_4 fluxes from the lakes and ponds in this area were much smaller than observations by Walter *et al.* (2006) in Siberia (18.7 gC m^{-2} yr^{-1}), probably because of the poorer SOC and colder climate conditions. However, these lakes and ponds could still be important sources of CH_4 flux observed by EC method. For example, the extremely high CH_4 flux observed by EC method on June 27, 2006 (DOY 178) was probably due to thawing and breaking of the lake/pond ice, which disturbed the bottom sediments and causing a release of the CH_4 stored in the bottom of the lakes or ponds (Sachs *et al.* 2008a). During the cold period in mid September (around DOY 255), all the chamber observations showed low CH_4 fluxes while noticeable CH_4 fluxes were measured by EC method. This was probably due to the contributions of the open water bodies as well. Atmosphere pressure was decreasing on DOY 178 and 255 (Figure 8), which could promote ebullition from the open water.

Secondly, the areal fraction of the inundated area may change with time. The aerial image used for land type classification was taken in August. The water table was higher and a larger area was inundated just after snow melting. Since we used constant areal fractions determined from the late growing season, this treatment may have underestimated CH_4 fluxes when water table is high, especially in the early growing season. Therefore more spatially detailed and temporally frequent images may be needed to reduce this error. In addition, the sources of CH_4 observed by the eddy tower might change with time due to the changes in footprint and wind direction. The average 80% cumulative footprint was 518 m during snow-free periods (Saches *et al.* 2008). Although the wet polygonal tundra extended more than 600 m in all directions from the eddy tower, the distributions of the land cover types, especially ponds and shallow lakes, differ slightly within the footprint of the EC observations (Figure 2c), which may cause some differences in EC observed fluxes due to variations in wind directions. Statistic analysis shows that EC observed CH_4 fluxes tend to be larger when wind is from south or from north than from other directions.

Thirdly, although we improved the model for ebullition emissions of CH_4, the eventful or episodic nature of ebullition (Tokida *et al.* 2007) and the atmospheric effects on diffusion of CH_4, especially we did not model emissions from open water, could cause mismatches between the modeled daily CH_4 fluxes and the EC observations. Sachs *et al.* (2008a) found that EC observed CH_4 fluxes were closely correlated with changes in friction velocity (which is related with wind velocity) and air pressure, probably due to reduction in boundary resistance and enhancement of ebullition. Our modeled daily CH_4 fluxes did not show strong correlations with wind speed and atmospheric pressure (more discussion in the next section). However, the correlation coefficient between the model upscaled and the EC observed CH_4 fluxes almost doubled if we used 3-day running averages comparing to the original daily fluxes. This result suggests that the atmospheric conditions probably mainly affect the short time (hours to several days) variations in CH_4 fluxes. The variation patterns of CH_4 flux in longer time (several days or longer) is mainly determined by soil processes (CH_4 production, consumption and transportation). Thus, our soil-based modeling approach (comparing to the atmospheric condition based approach, such as the equation developed by Sachs *et al.* (2008a)) can generally capture the magnitudes and the long-term patterns of the CH_4 fluxes but may miss some short term variations due to the impacts of atmospheric conditions on CH_4 transport processes.

4.3 Major controls of CH_4 fluxes on plant community and ecosystem scales

Our model results for different land types indicated that water table depth was the most important factor controlling CH_4 fluxes. The annual total CH_4 fluxes differed by about one order of magnitude per unit area between the inundated land types (Types I, II and II) and the non-inundated land types (Types IV and V). Several studies have indicated that CH_4 fluxes are high in inundated conditions but decrease significantly when water table is 5 cm or more below the land surface (e.g., Morrissey & Livingston 1992). Soil moisture conditions were important for the non-inundated land types as well. As for seasonal variations, air or near surface soil temperatures were closely correlated with CH_4 fluxes for the inundated land types (correlation coefficients were 0.62-0.74 between the modeled daily CH_4 fluxes and air temperature, and 0.70-0.83 between the modeled daily CH_4 fluxes and soil temperature at 5 cm depth for the three chamber observation sites during the EC observation period). This result is in agreement with Sachs *et al.* (2010) who found close correlations between chamber measured daily CH_4 fluxes and the soil surface temperature. This is because water table was usually above the land surface in this land type, and the major controls of CH_4 fluxes were CH_4 production and transport to the atmosphere, which were mainly dependent on temperature constrained microbial activities and plant growth in this cold region. For the non-inundated land types, modeled daily CH_4 emissions occurred when soil was thawed but the correlation with soil temperature was low (0.11 and 0.44 for chamber site 2 and 5, respectively, during the EC observation period). Daily CH_4 fluxes seem responded to the fluctuations of water table, but the correlation was not very high (0.45 and 0.41 for chamber sites 2 and 5, respectively, for the EC observation period), probably because the soil moisture conditions above the saturated zone is more important when water table is low. The fluctuation of the modeled daily CH_4 fluxes sometimes corresponded to changes in atmosphere pressure due to its impacts on ebullition, especially during the mid growing season (Figure 8a). The correlation coefficient, however, was not significant (-0.21 for the mid growing season period (DOY 185-250, or July 4 to Sept. 7, 2006), but 0.21 for the EC observation period), probably due to the effects of other factors (e.g., water table, temperature, and solar radiation, etc).

At ecosystem scale, the inundated land types were the major contributors to CH_4 fluxes. Therefore the flux rates and areal fractions of different plant communities are critical for the total CH_4 fluxes at the ecosystem scale. The modeled ecosystem CH_4 fluxes (i.e., the modeled area-weighted average CH_4 fluxes from all the land types) were correlated with the daily soil temperature at 5cm depth in the wet low-centered polygons (the correlation coefficient was 0.63 for the EC observation period). The fluctuation of the modeled ecosystem CH_4 fluxes also corresponded to changes in atmosphere pressure, especially during the mid growing season (Figure 8b), but the correlation coefficient was low (-0.25 for the mid growing season period (DOY 185-250, or July 4 to Sept. 7, 2006) but 0.22 for the EC observation period). This was similar to the correlations for the inundated land types since they were the major contributors to the ecosystem CH_4 fluxes.

In summary, this study integrated a biogeochemical model with a permafrost model so that the new model is suitable to simulating biogeochemical processes in high latitudes. The new model possesses several improved features, including upscaling from plant communities to the ecosystem scale and a new ebullition module based on the ideal gas law and Henry's law, with which the effects of water level, temperature, thawing/freezing and atmospheric pressure on ebullition were integrated. Model tests showed that the simulated soil temperature and thaw depths were in agreement with observations at a polygonal permafrost area. The modeled CH_4 fluxes at five different sites were close to the chamber observations. The modeled area-weighted average CH_4 fluxes were similar to the EC observations in temporal pattern and in the annual total although discrepancies existed on short time scales. These tests suggest that the model is capable to quantify the biophysical and biogeochemical processes at plant community scale, and from which CH_4 fluxes at ecosystem scale can be estimated.

Acknowledgements

The authors would like to thank Drs. Ian Olthof and Wenjun Chen for their critical internal review of the paper. The comments and suggestions from two journal reviewers are very helpful to improve the manuscript. This study is supported by a NASA project on northern high latitude wetland carbon dynamics (08-TE08-0013), the climate change geoscience program in Natural Resources Canada (the contribution number is 20110086), a GRIP project (ParkSPACE) funded by Canadian Space Agency, and Canada's IPY funding (CiCAT).

References

Aber JD, and Federer CA (1992) A generalized, lumped-parameter model of photosynthesis, evaporation and net primary production in temperate and boreal forest ecosystems. *Oecologia*, **92**, 463–474.

Are FE, Reimnitz E (2000) An overview of the Lena River Delta setting: geology, tectonics, geomorphology, and hydrology. *Journal of Coastal Research*, **16**(4), 1083-1093.

Baird AJ, Beckwith CW, Waldron S, Waddington JM (2004). Ebullition of methane-containing gas bubbles from near-surface sphagnum peat. *Geophysical Research Letters*, **31**, L21505.

Beckmann MS, Sheppard K, Lloyd D (2004) Mass spectrometric monitoring of gas dynamics in peat monoliths: effects of temperature and diurnal cycles on emissions. *Atmospheric Environment*, **38**, 6907-6913.

Boike J, Wille C, Abnizova A (2008) Climatology and summer energy and water balance of polygonal tundra in the Lena River Delta, Siberia. *Journal of Geophysical Research,* **113**(G03025).

Bubier J, Costello A, Moore TR, Roulet NT, Savage K (1993) Microtopography and methane flux in boreal peatlands, northern Ontario, Canada. *Canadian Journal of Botany,* **71**, 1056-1063.

Cao M, Marshall S (1988) Global methane emission from wetlands and its sensitivity to climate change. *Atmospheric Environment*, **32**, 3293-3299.

Chen W, Li J, Zhang Y *et al.* (2009) Relating biomass and leaf area index to non-destructive measurements in order to monitor changes in arctic vegetation. *Arctic*, **62**, 281-294.

Christensen TR, Panikov, N, Mastepanov M *et al.* (2003) Biotic controls on CO_2 and CH_4 exchange in wetlands - A closed environment study. *Biogeochemistry*, **64**, 337-354.

Dinsmore KJ, Skiba UM, Billett MF, Rees RM, Drewer J (2009) Spatial and temporal variability in CH_4 and N_2O fluxes from a Scottish ombrotrophic peatland: Implications for modelling and up-scaling. *Soil Biology and Biochemistry,* **41**, 1315–1323.

Fechner-Levy FJ, Hemond HF (1996) Trapped methane volume and potential effects on methane ebullition in a northern peatland. *Limnololy and Oceanography*, **41**(7), 1375-1383.

Frolking S, Roulet NT, Lawrence D (2009) Issues related to incorporating northern peatlands into global climate models. In: *Northern Peatlands and Carbon Cycling* (eds Baird A, Belyea L, Comas X, Reeve A, Slater L), pp.19-35. Geophysical Monograph 184, American Geophysical Union, Washington DC.

Fumoto F, Kobayashi K, Li C, Yagi K, Hasegawa T (2008) Revising a process-based biogeochemistry model (DNDC) to simulate methane emission from rice paddy fields under various residue management and fertilizer regimes. *Global Change Biology,* **14**, 382-402.

Giltrap, DL, Li C, Saggar S (2010) DNDC: A process-based model of greenhouse gas fluxes from agricultural soils. *Agriculture, Ecosystems and Environment*, **136**, 292-230.

Glaser PH, Chanton JP, Morin P, Rosenberry DO, Siegel DI, Ruud O, Chasar LI, Reeve AS (2004) Surface deformations as indicators of deep ebullition fluxes in a large northern peatland. *Global Biogeochemical Cycles,* **18**, GB1003.

Grant B, Smith WN, Desjardins R, Lemke R, Li C (2004) Estimated N_2O and CO_2 emissions as influenced by agricultural practices in Canada. *Climatic Change,* **65**, 315-332.

Hargreaves KJ, Fowler D, Pitcairn CER, Aurela M (2001) Annual methane emission from Finnish mires estimated from eddy covariance campaign measurements. *Theoretical and Applied Climatology*, **70**, 203-213.

Heikkinen JEP, Maljanen M, Aurela M, Hargreaves KJ, Martikainen PJ (2006) Carbon dioxide and methane dynamics in a sub-Arctic peatland in northern Finland. *Polar Research,* **21**(1), 49–62.

Hendriks DMD, van Huissteden J, Dolman AJ (2010) Multi-technique assessment of spatial and temporal variability of methane fluxes in a peat meadow. *Agricultural and Forest Meteorology,* **150**, 757–774.

Kellner E, Baird AJ, Oosterwoud M, Harrison K, Waddington JM (2006) Effect of temperature and atmospheric pressure on methane (CH_4) ebullition from near-surface peats. *Geophysical Research Letters*, **33**, L18405.

Kutzbach L, Wagner D, Pfeiffer E (2004) Effect of microrelief and vegetation on methane emission from wet polygonal tundra, Lena Delta, Northern Siberia. *Biogeochemistry,* **69**, 341–362.

Lelieveld J, Crutzen P, Dentener DJ (1998) Changing concentration, lifetime and climate forcing of atmospheric methane. *Tellus,* **5B**, 128–150.

Li C, Qiu J, Frolking S *et al.* (2002) Reduced methane emissions from large scale changes in water management of China's rice paddies during 1980–2000. *Geophysical Research Letters*, **29**(20), 1972.

Li C, Aber J, Stange F, Butterbach-Bahl K, Papen H (2000) A process-oriented model of N_2O and NO emissions from forest soils: 1. Model development. *Journal of Geophysical Research,* **105**, 4369-4384.

Li C, Frolking S, Frolking TA (1992) A model of nitrous oxide evolution from soil driven by rainfall events: 1. Model structure and sensitivity. *Journal of Geophysical Research,* **97**(D9), 9759–9776.

Liss PS, Slater P (1974) Flux of gases across the air-sea interface. *Nature*, **247**, 181–184.

Kobabe S, Wagner D, Pfeiffer E (2004) Characterisation of microbial community composition of a Siberian tundra soil by fluorescence in situ hybridisation. *FEMS Microbiology Ecology,* **50**, 13–23.

Mastepanov M, Sigsgaard C, Dlugokencky EJ, Houweling S, Ström L, Tamstorf MP, Christensen TR (2008) Large tundra methane burst during onset of freezing. *Nature* **456**, 628-630.

Matthews E, Fung I (1987) Methane emission from natural wetlands: Global distribution, area, and environmental characteristics of sources. *Global Biogeochemical Cycles*, ***1***(1), 61–86.

Moore TR, Knowles R (1990) Methane emissions from fen, bog and swamp peatlands in Quebec. *Biogeochemistry*, **11**, 45-61.

Morrissey LA, Livingston GP (1992) Methane emissions from Alaska arctic tundra: An assessment of local spatial variability. *Journal of Geophysical Research*, ***97***(D15), 16, 661–16, 670.

Muster S, Langer M, Heim B, Westermann S, Boike J (submitted) Scaling land cover of Arctic polygonal tundra and its effect on evapotranspiration. *Tellus*.

Pollack HN, Hurter SJ, Johnson JR (1991). Heat flow from the earth's interior: analysis of the global data set. *Reviews of Geophysics*, **31**, 267-280.

Prather M, et al. (2001) Atmospheric chemistry and greenhouse gases, in: *Climate Change 2001: The Scientific Basis—Contribution of Working Group I to the Third Assessment Report of the Intergovernmental Panel on Climate Change*, (eds Houghton JT et al.), pp. 239– 287, Cambridge University Press, New York.

Price JS (2003) The role and character of seasonal peat soil deformation on the hydrology of undisturbed and cutover peatlands. *Water Resources Research*, **39**(9), 1241, doi:10.1029/2002WR001302.

Riutta T, Laine J, Aurela M et al. (2007) Spatial variation in plant community functions regulates carbon gas dynamics in boreal fen ecosystem. *Tellus,* **59B** 838-852.

Rosenberry DO, Glaser PH, Siegel DI (2006) The hydrology of northern peatlands as affected by biogenic gas: current developments and research needs. *Hydrological Processes,* **20**, 3601–3610

Sachs T, Wille C, Boike J, Kutzbach L (2008a) Environmental controls on ecosystem-scale CH_4 emission from polygonal tundra in the Lena River Delta, Siberia. *Journal of Geophysical Research*, **113**, G00A03.

Sachs T, Giebels M, Wille C, Kutzbach L, Boike J (2008b) Methane emission from Siberian wet polygonal tundra on multiple spatial scales: vertical flux measurements by closed chambers and eddy covariance, Samoylov Island, Lena River Delta. In: *Ninth International Conference on Permafrost*, Institute of Northern Engineering (eds Kane DL, Hinkel KM), p1549-1554. University of Alaska Fairbanks.

Sachs T, Giebels M, Boike J, Kutzbach L (2010) Environmental controls of CH_4 emission from polygonal tundra on the micro-site scale, Lena River Delta, Siberia. *Global Change Biology,* **16**(11), 3096-3110.

Schneider J, Grosse G, Wagner D (2009) Land cover classification of tundra environments in the arctic Lena Delta based on Landsat 7 ETM+ data and its application for upscaling of methane emissions. *Remote Sensing of Environment,* **113**, 380–391.

Schrier-Uijl AP, Kroon PS, Hensen A, Leffelaar PA, Berendse F, Veenendaal EM (2010) Comparison of chamber and eddy covariance-based CO_2 and CH_4 emission estimates in a heterogeneous grass ecosystem on peat. *Agricultural and Forest Meteorology,* **150**, 825–831.

Spott O (2003) *Polygonal tundra lakes and their function as sources of atmospheric methane*. Diploma thesis, University of Leipzig, 137pp (in German).

Strack M, Kellner E, Waddington JM (2005) Dynamics of biogenic gas bubbles in peat and their effects on peatland biogeochemistry. *Global Biogeochemical Cycles*, **19**, GB1003.

Tarnocai C, Canadell JG, Schuur EAG, Kuhry P, Mazhitova G, Zimov S (2009) Soil organic carbon pools in the northern circumpolar permafrost region. *Global Biogeochemical Cycles*, **23**, GB2023.

Tokida T, Mizoguchi M, Miyazaki T, Kagemoto A, Nagata O, Hatano R (2007) Episodic release of methane bubbles from peatland during spring thaw. *Chemosphere*, **70**, 165–171.

Tokida T, Miyazaki T, Mizoguchi M (2005) Ebullition of methane from peat with falling atmospheric pressure. *Geophysical Research Letters*, **32**, L13823.

Wagner D, Lipski A, Embacher A, Gattinger A (2005) Methane fluxes in permafrost habitats of the Lena Delta: effects of microbial community structure and organic matter quality. *Environmental Microbiology,* **7**(10), 1582–1592.

Walter KM, Zimov SA, Chanton JP, Verbyla D, Chapin III FS (2006) Methane bubbling from Siberian thaw lakes as a positive feedback to climate warming. *Nature,* **443***,* 71–75.

Walter BP, Heimann M (2000) A process-based, climate-sensitive model to derive methane emissions from natural wetlands: Application to five wetland sites, sensitivity to model parameters, and climate. *Global Biogeochemical Cycles*, **14**(3), 745–765.

Walter BP, Heimann M, Matthews E (2001) Modeling modern methane emissions from natural wetlands: 1. Model description and results. *Journal of Geophysical Research*, **106**(D24), 34,189– 34,206.

Wagner D, Lipski A, Embacher A, Gattinger A (2005) Methane fluxes in permafrost habitats of the Lena Delta: effects of microbial community structure and organic matter quality. *Environmental Microbiology,* **7**, 1582–1592.

Whalen S, Reeburgh WS, Kizer KS (1991) Methane consumption and emission by taiga. *Global Biogeochemical Cycles*, **5**(3), 261–273.

Yu Z, Loisel J, Brosseau DP, Beilman DW, Hunt SJ (2010) Global peatland dynamics since the Last Glacial Maximum. *Geophysical Research Letters*, **37**, L13402.

Zhang Y, Chen W, Riseborough DW (2008a) Disequilibrium response of permafrost thaw to climate warming in Canada over 1850-2100. *Geophysical Research Letters,* **35**, L02502.

Zhang Y, Chen W, Riseborough DW (2008b) Modeling the long-term dynamics of snow and their impacts on permafrost in Canada. In: *Ninth International Conference on Permafrost* (eds Kane DL, Hinkel KM), p2055-2060. Institute of Northern Engineering, University of Alaska Fairbanks.

Zhang Y, Chen W, Smith SL, Riseborough DW, Cihlar J (2005) Soil temperature in Canada during the twentieth century: complex responses to atmospheric climate change. *Journal of Geophysical Research,* **110**, D03112.

Zhang Y, Chen W, Cihlar J (2003) A process-based model for quantifying the impact of climate change on permafrost thermal regimes. *Journal of Geophysical Research,* **108**(D22), 4695.

Zhang Y, Li C, Trettin CC, Li H, Sun G (2002a) An integrated model of soil, hydrology and vegetation for carbon dynamics in wetland ecosystems. *Global Biogeochemical Cycles,* **16**(4), 1061.

Zhang Y, Li C, Zhou X, Moore III B (2002b) A simulation model linking crop growth and soil biogeochemistry for sustainable agriculture. *Ecological Modelling,* **151**, 75-108.

Zhuang Q, Melillo JM, Kicklighter DW *et al.* (2004) Methane fluxes between terrestrial ecosystems and the atmosphere at northern high latitudes during the past century: A retrospective analysis with a process-based biogeochemistry model. *Global Biogeochemical Cycles*, **18**, GB3010.

Table 1 Soil profiles for the polygon centers and polygon rims. The data are from Kutzbach *et al.* (2004) and Wagner *et al.* (2005).

Depth (cm)	Texture	SOC (%)	C/N ratio	Bulk density (g cm^{-3})	pH
Polygon centers					
0-11	Peat	22.1	43	0.4	7.9
11-26	Peat with sand	12.6	35	0.6	7.4
26-31	Sand	4.1	100	0.82	7.4*
31-64	Sandy loam	4.2	30	0.82*	7.4*
Polygon rims					
0-15	Loamy Sand	1.8	21	1.06	7.9*
15-18	Sandy loam	2.2	21	1.21	7.9
18-32	Loam	3.4	25	1.23	6.7
32-46	Loam	2.3	22	1.35	6.7*
46-90	Loam	3.0	20	1.35*	6.7*

*Not observed and was assumed as the same as the above layer.

Table 2 The input data for leaf area index and above-ground biomass. They were estimated based on the equations developed by Chen *et al.* (2009) according to the coverage and height observations from Kutzbach *et al.* (2004)

Vegetation	Parameters	Low centers	Rims
Sedges	Above-ground biomass (kg C/ha)	146.3	27.9
	Leaf area index	0.29	0.06
Shrubs	Above-ground biomass (kg C/ha)	0	214.8
	Leaf area index	0	0.21
Mosses	Biomass of mosses (kg C/ha)	802.9	802.9

Table 3 Hydrological parameters for lateral flows and snow drifting of different land types (Calibrated based on observed water table depth at different sites. Land types II to V are overgrown water, wet low-centered polygons, moist high-centered polygons, and polygon rims, respectively)

Parameters*	Type II	Type III	Type IV	Type V
Surface inflow rate	0.3	0.1	0.0	0.0
Surface outflow depth (m)	-0.2	0.0	0.05	0.1
Surface outflow rate	0.01	0.0	0.5	0.5
Ground outflow depth (m)	0.1	0.0	0.5	0.5
Ground outflow rate	0.001	0.0	0.0025	0.0025
Snow drifting factor	-0.2	0.0	0.25	0.5

* Surface inflow rate is the fraction of rainfall (or water from snow melting) added to the site from its surroundings. The surface outflow depth is the lowest water table depth (positive for below the land surface, and negative for above the land surface) above which lateral outflow occurring. The surface outflow rate is the fraction of water table above the lowest depth will be lost as lateral outflow in a day. The definitions for ground outflow depth and rate were similar as that for surface outflow (See Zhang *et al.* (2002a) for details). The snow drifting factor was the fraction of daily snowfall blown away from the site (a negative value means snowfall blown into the site from its surroundings).

Captions

Figure 1. The structure of the NEST-DNDC model developed based on the DNDC model (Zhang *et al.* 2002a, Li *et al.* 2000) and the NEST model (Zhang *et al.*, 2003). Solid lines are for matter flows, and dashed lines are for information flow. Rectangles are for major state variables, circles are for gases could release to the atmosphere, and the octagon is for CH_4 in bubbles.

Figure 2. The location of the study area. a) the location of the Lena River Delta (marked by a red square) in the arctic map (from UNEP/GRID-Arendal Maps and Graphics Library, 2006). b) the location of the Samoylov Island (marked by a red rectangle) in the Lena river delta (Landsat 7 satellite image from NASA and U.S. Geological Survey). c) an aerial image show the location of the field observation area (marked by a red rectangle) in the Samoylov Island. d) the chamber and EC observation sites (sites 1, 3 and 4 are in wet low-centered polygons, site 2 is in a high-centered polygon, and site 5 is at polygon rim. EC tower is at site 6, and site 7 is for a tent and equipment).

Figure 3. Comparisons between modeled and observed soil temperature at different depths a) at a low-center and b) at polygon rims, and c) summer thaw depth (c). The low-center was simulated based on chamber site 1 using measured water table. The results for other low-centers (sites 3 and 4) were similar to that of the site 1.

Figure 4. Modeled water table dynamics and comparisons between simulated and measured CH_4 fluxes at the five chamber observation sites. The circles are observed and the curves are modeled. Water table was modeled when there were no observations; otherwise observed water table was used during simulation (negative water table depth is for water level above the land surface).

Figure 5. Scatter-graph comparisons between modeled and measured CH_4 fluxes at the five chamber observation sites (a-e) and between the modeled area-weighted average CH_4 fluxes and the EC measured CH_4 fluxes (R is correlation coefficient and n is the number of days with observations).

Figure 6. Comparisons between the modeled area-weighted average CH_4 fluxes (the curves) and the EC observed CH_4 fluxes (the circles).

Figure 7 Comparison between the modeled and observed water-table at three wet low-centered polygons (Land type III) (negative water table depth is for water level above the land surface).

Figure 8. Variations of atmospheric pressure (curves with circles) and modeled CH_4 fluxes (curves with dotes) at plant community scale (chamber site 1) and at ecosystem scale.

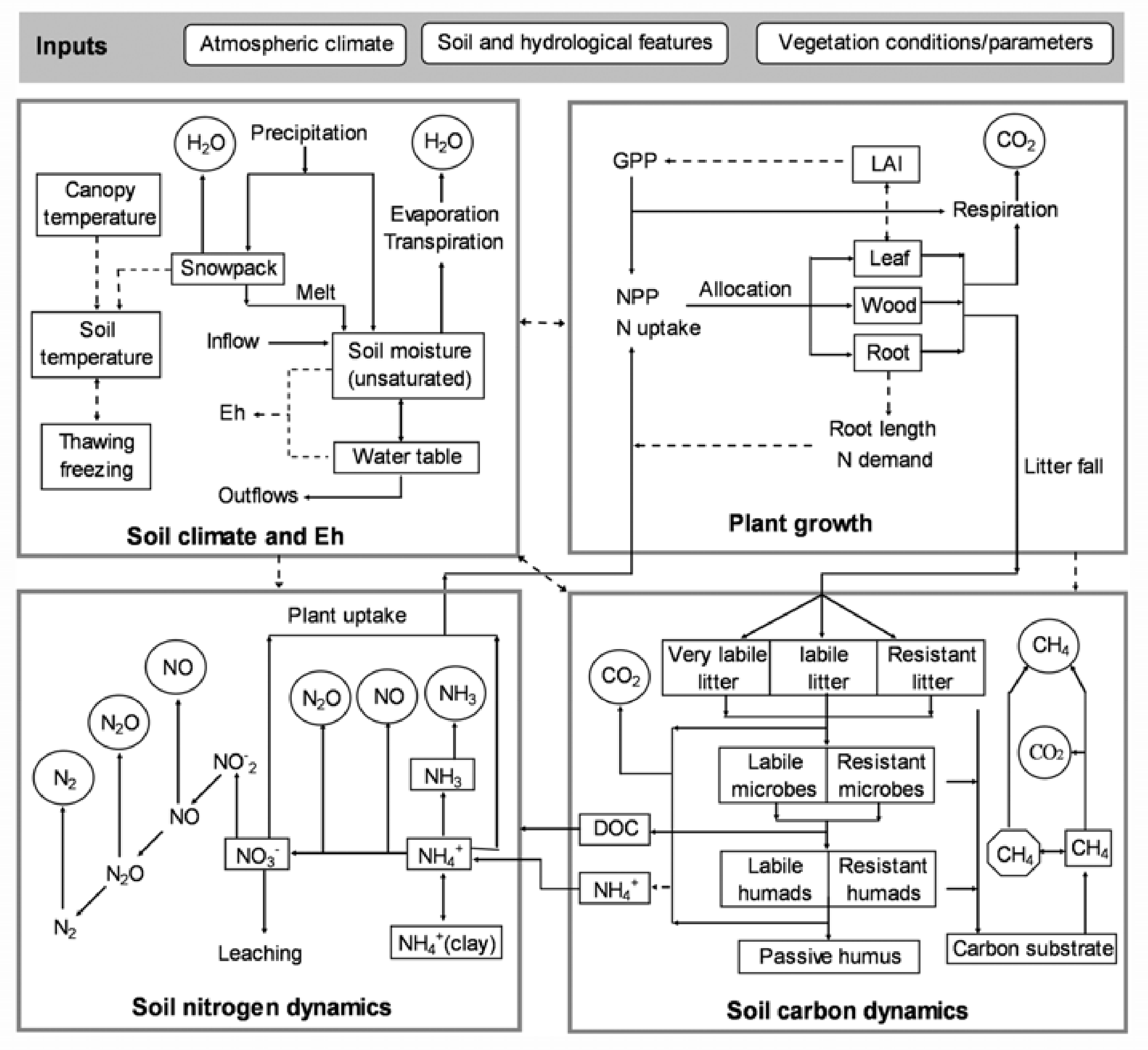
Inputs
Atmospheric climate
Soil and hydrological features
Vegetation conditions/parameters
H_2O
Precipitation
H_2O
Canopy temperature
Snowpack
Evaporation
Transpiration
Melt
Soil temperature
Inflow
Soil moisture (unsaturated)
Eh
Thawing freezing
Water table
Outflows
Soil climate and Eh
GPP
LAI
CO_2
Respiration
Leaf
NPP
Allocation
Wood
N uptake
Root
Root length
N demand
Litter fall
Plant growth
Plant uptake
NO
N_2O
N_2O
NO
NH_3
N_2
NO^-_2
NH_3
NO
N_2O
NO_3^-
NH_4^+
DOC
N_2
NH_4^+
Leaching
NH_4^+(clay)
Soil nitrogen dynamics
CO_2
Very labile litter
labile litter
Resistant litter
CH_4
CO_2
Labile microbes
Resistant microbes
CH_4
CH_4
Labile humads
Resistant humads
Passive humus
Carbon substrate
Soil carbon dynamics

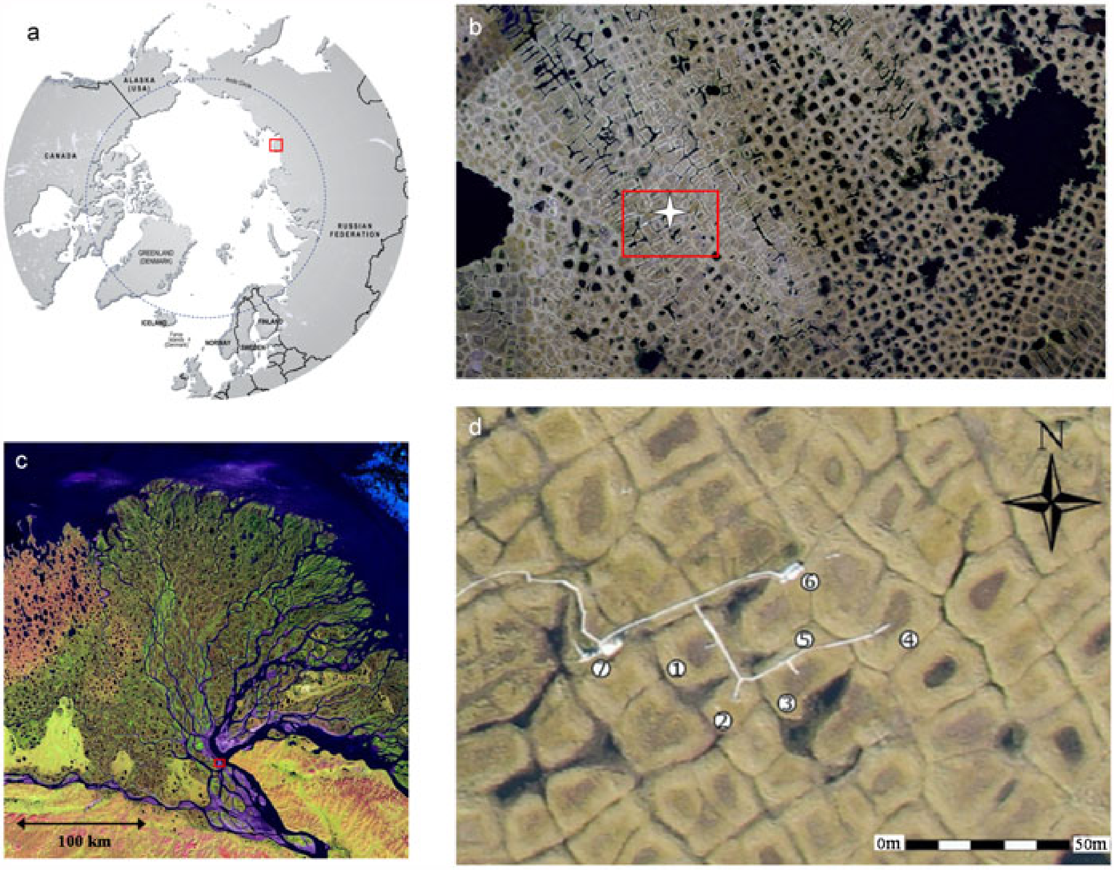
a
ALASKA (USA)
CANADA
GREENLAND (DENMARK)
ICELAND
NORWAY
SWEDEN
FINLAND
RUSSIAN FEDERATION
b
c
100 km
d
N
⑥
⑤
④
⑦
①
③
②
0m
50m

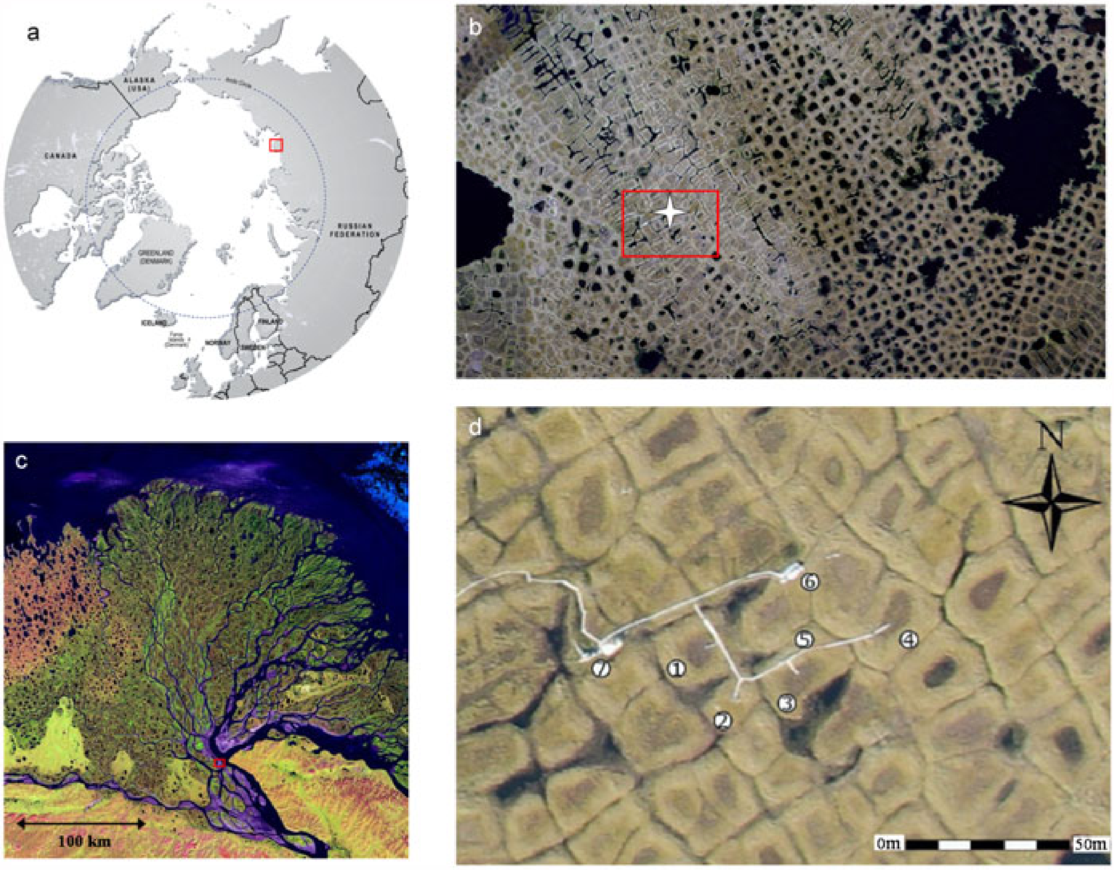
a
ALASKA (USA)
CANADA
GREENLAND (DENMARK)
RUSSIAN FEDERATION
ICELAND
NORWAY
SWEDEN
FINLAND
b
c
100 km
d
N
⑥
⑤
④
⑦
①
②
③
0m
50m

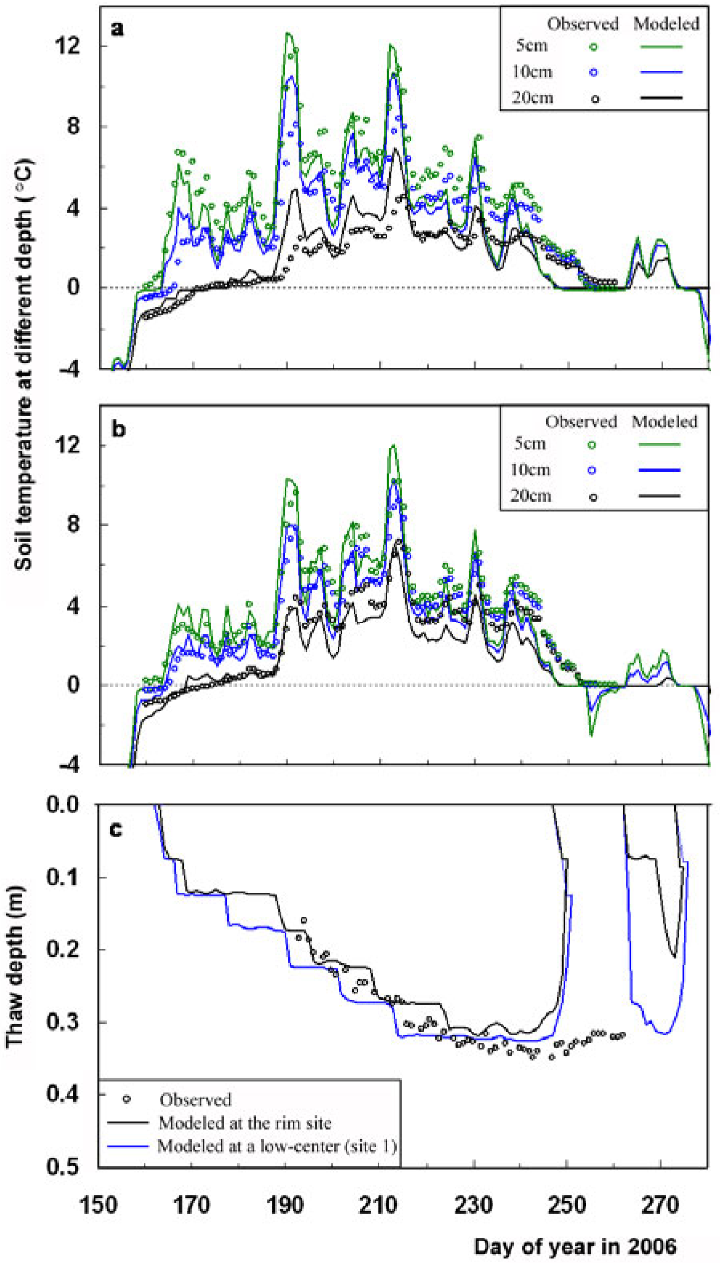
a
Observed
Modeled
5cm
10cm
20cm
b
Observed
Modeled
5cm
10cm
20cm
c
Observed
Modeled at the rim site
Modeled at a low-center (site 1)
Soil temperature at different depth (°C)
12
8
4
0
-4
Thaw depth (m)
0.0
0.1
0.2
0.3
0.4
0.5
150
170
190
210
230
250
270
Day of year in 2006

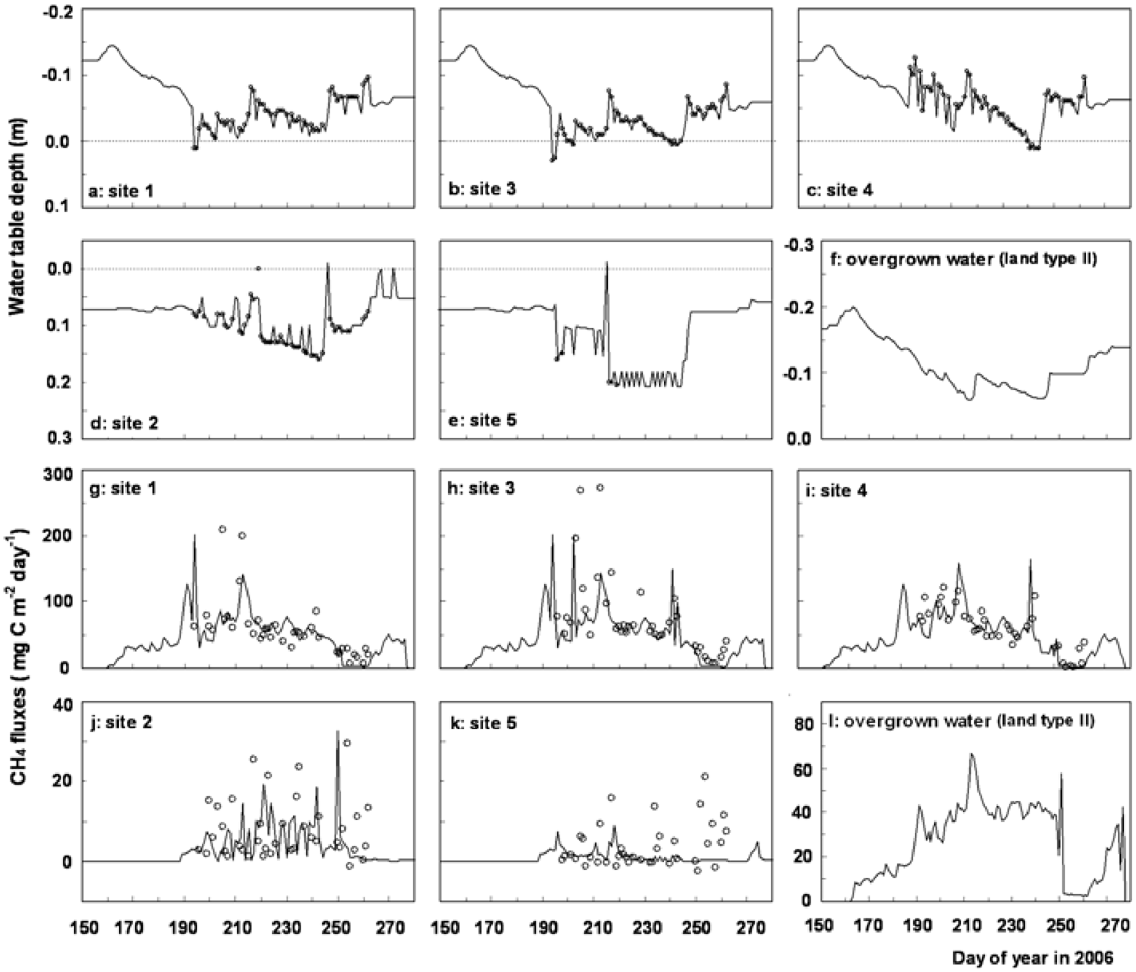

Water table depth (m)
-0.2
-0.1
0.0
0.1
a: site 1
b: site 3
c: site 4
0.0
0.1
0.2
0.3
d: site 2
e: site 5
-0.3
-0.2
-0.1
0.0
f: overgrown water (land type II)
CH₄ fluxes (mg C m⁻² day⁻¹)
300
200
100
0
g: site 1
h: site 3
i: site 4
40
20
0
j: site 2
k: site 5
80
60
40
20
0
l: overgrown water (land type II)
150
170
190
210
230
250
270
Day of year in 2006

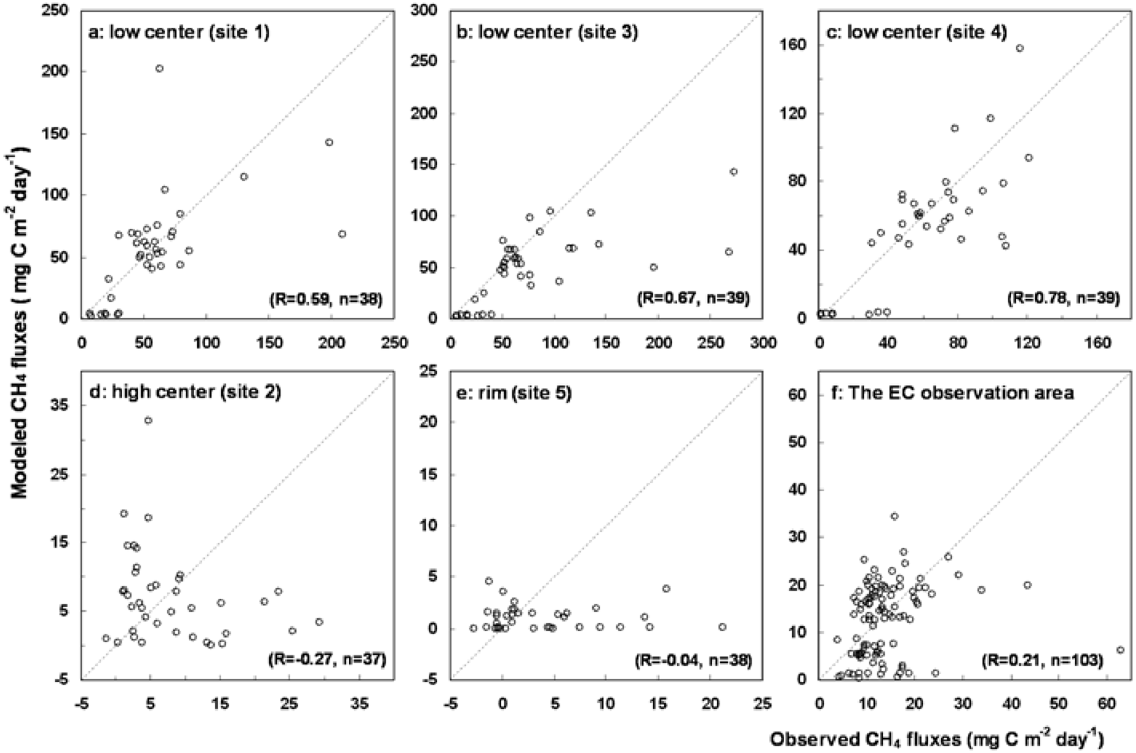
a: low center (site 1)
(R=0.59, n=38)
b: low center (site 3)
(R=0.67, n=39)
c: low center (site 4)
(R=0.78, n=39)
d: high center (site 2)
(R=-0.27, n=37)
e: rim (site 5)
(R=-0.04, n=38)
f: The EC observation area
(R=0.21, n=103)
Modeled CH4 fluxes (mg C m-2 day-1)
Observed CH4 fluxes (mg C m-2 day-1)

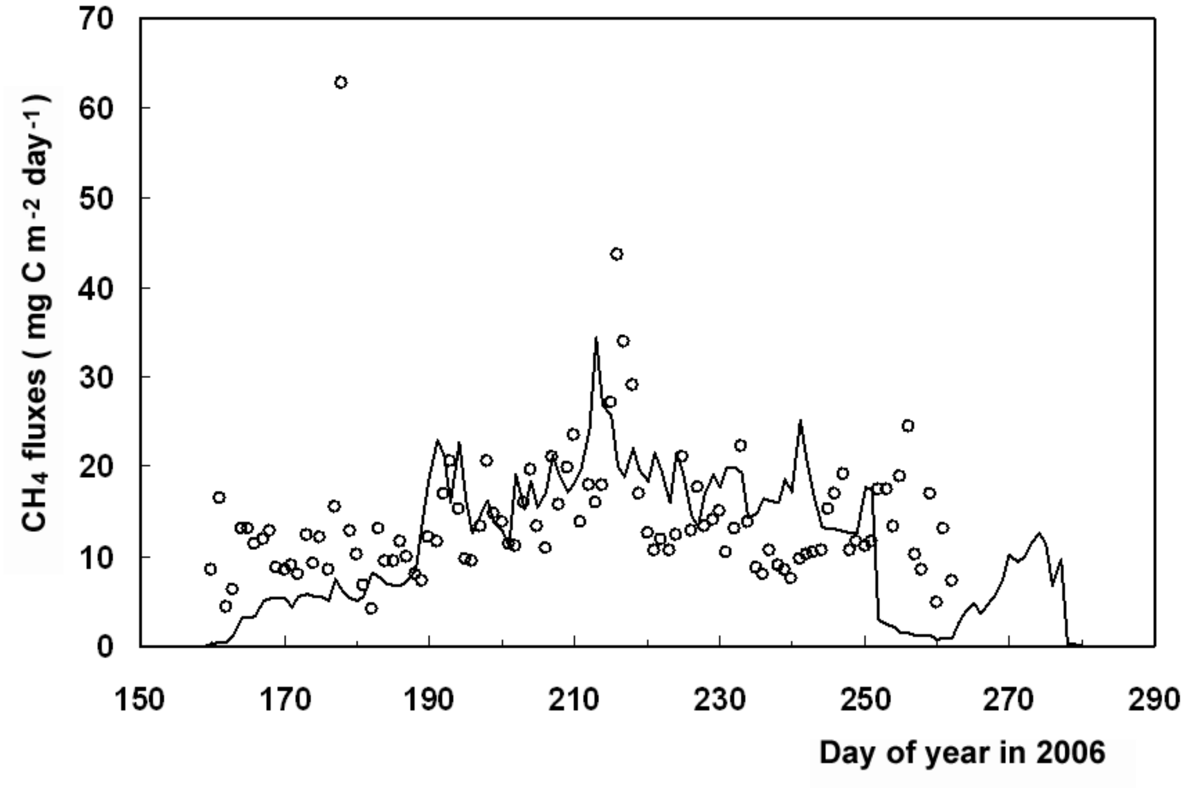

70
60
50
40
30
20
10
0
CH$_4$ fluxes (mg C m^{-2} day^{-1})
150
170
190
210
230
250
270
290
Day of year in 2006

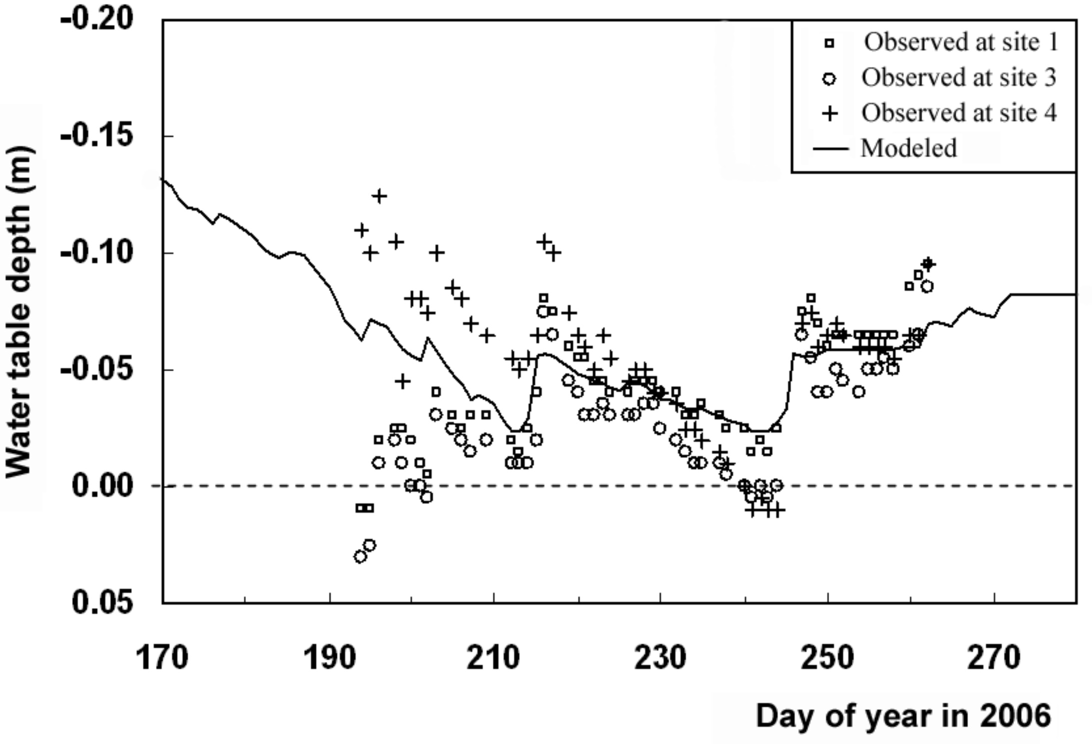
Water table depth (m)
-0.20
-0.15
-0.10
-0.05
0.00
0.05
170
190
210
230
250
270
Day of year in 2006
Observed at site 1
Observed at site 3
Observed at site 4
Modeled

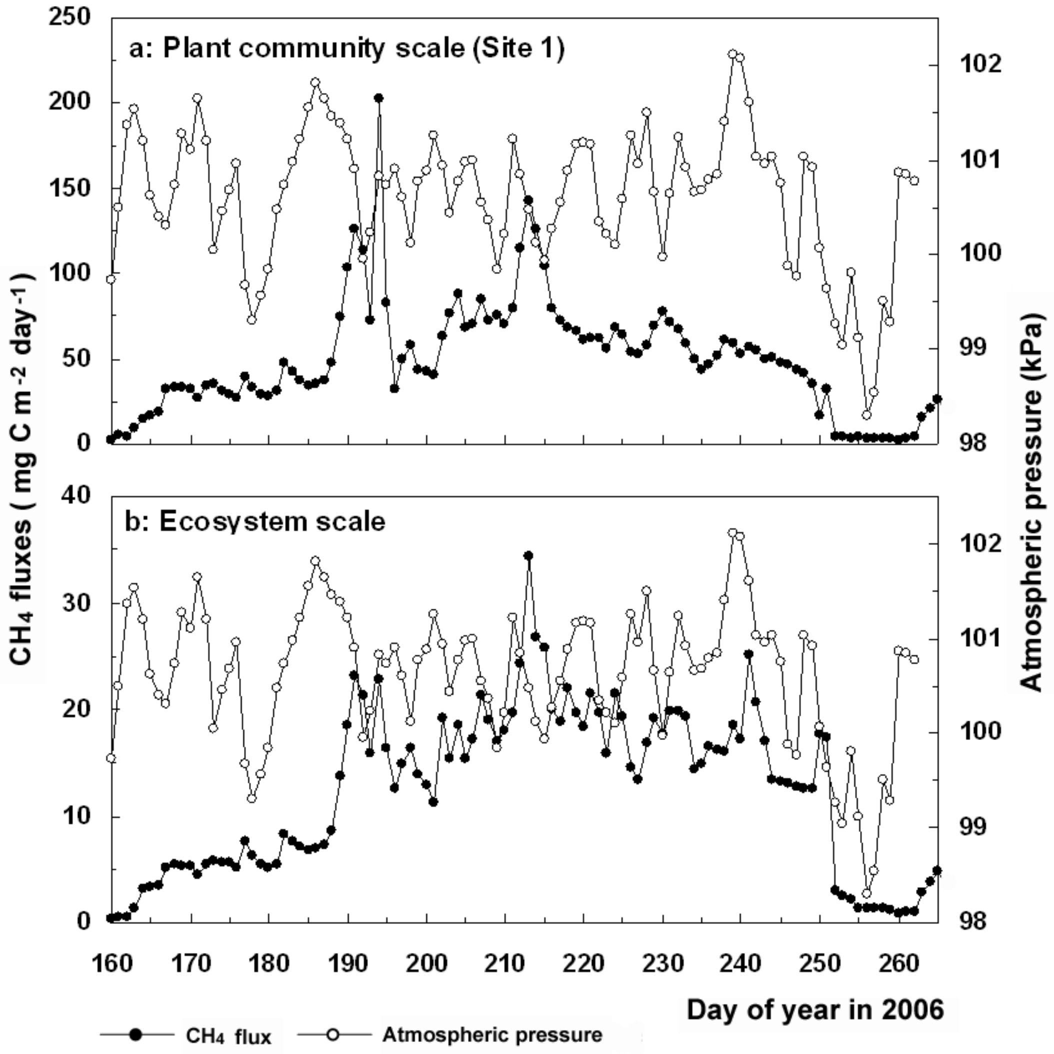
a: Plant community scale (Site 1)
b: Ecosystem scale
CH₄ fluxes (mg C m-2 day-1)
Atmospheric pressure (kPa)
0
50
100
150
200
250
0
10
20
30
40
98
99
100
101
102
160
170
180
190
200
210
220
230
240
250
260
Day of year in 2006
CH₄ flux
Atmospheric pressure